Journal of Computational Mathematics
Vol.xx, No.x, 2023, 1–20.

http://www.global-sci.org/jcm
doi:10.4208/jcm.2307-m2022-0225

STABLE RECOVERY OF SPARSE SIGNALS WITH NON-CONVEX WEIGHTED r-NORM MINUS 1-NORM*

Jianwen Huang
School of Mathematical Sciences, Chongqing Normal University, Chongqing 401331, China
School of Mathematics and Statistics, Tianshui Normal University, Tianshui 741001, China
Email: hjw1303987297@126.com
Feng Zhang[1)]
School of Mathematics and Statistics, Southwest University, Chongqing 400715, China
Email: zfmath@swu.edu.cn
Xinling Liu
Key Laboratory of Optimization Theory and Applications at China West Normal University of Sichuan Province, School of Mathematics and Information, China West Normal University, Nanchong 637009, China
Email: fsliuxl@163.com
Jianjun Wang
School of Mathematics and Statistics, Southwest University, Chongqing 400715, China
School of Mathematics and Information Science, North Minzu University, Yinchuan 750021, China
Email: wjj@swu.edu.cn
Jinping Jia
School of Mathematics and Statistics, Tianshui Normal University, Tianshui 741001, China
Email: jjping2006@163.com
Runke Wang
College of Resources and Environmental Engineering, Tianshui Normal University, Tianshui 741001, China
Email: wrk0531@tsnu.edu.cn

Abstract

Given the measurement matrix A and the observation signal y, the central purpose of compressed sensing is to find the most sparse solution of the underdetermined linear system $y = Ax + z$, where x is the s-sparse signal to be recovered and z is the noise vector. Zhou and Yu [Front. Appl. Math. Stat., 5 (2019), Article 14] recently proposed a novel non-convex weighted $\ell_r - \ell_1$ minimization method for effective sparse recovery. In this paper, under newly coherence-based conditions, we study the non-convex weighted $\ell_r - \ell_1$ minimization in reconstructing sparse signals that are contaminated by different noises. Concretely, the results reveal that if the coherence μ of measurement matrix A fulfills

$$\mu < \kappa(s; r, \alpha, N), \quad s > 1, \quad \alpha^{\frac{1}{r}} N^{\frac{1}{2}} < 1,$$

then any s-sparse signals in the noisy scenarios could be ensured to be reconstructed robustly by solving weighted $\ell_r - \ell_1$ minimization non-convex optimization problem. Furthermore, some central remarks are presented to clear that the reconstruction assurance is much weaker than the existing ones. To the best of our knowledge, this is the first mutual coherence-based sufficient condition for such approach.

Mathematics subject classification: 68W40, 68P30, 94A08, 94A12.
Key words: Compressed sensing, Sparse recovery, Mutual coherence, Sufficient condition.

* Received October 10, 2022 / Revised version received February 12, 2023 / Accepted July 4, 2023 / Published online December 14, 2023 /
1) Corresponding author

1. Introduction

Compressed sensing [3, 8] has recently triggered much interest in signal and imaging processing, statistics and applied mathematics. The crucial aim is to recover a high-dimensional sparse signal from a small quantity of linear measurements. Generally, one thinks about the linear model

$$y = Ax + z, \tag{1.1}$$

where $A \in \mathbb{R}^{m\times N}$ is the measurement matrix with $m \ll N$, $z \in \mathbb{R}^m$ is the noise vector and $x \in \mathbb{R}^N$ is an s-sparse (i.e. the number of nonzero elements of x is not more than s) vector to be recovered. Two widely utilized types of noises are the bounded ℓ_2 noise [9, 15] and the Dantzig selector noise [4], respectively. Throughout the article, we suppose that the columns of A are standardized, i.e. for all i, $A_i^\top A_i = 1$, where $A_i, 1 \le i \le N$, denotes the i-th column of A.

Because the linear model (1.1) is an underdetermined linear system, it is impossible to stably reconstruct x based on A, z and y. Fortunately, it is possible to stably reconstruct s-sparse signal x from (1.1) with a few appropriately exploiting sparse reconstruction methods under suitable assumptions regarding A and z. There are two extensively applied frameworks to describe such assumptions concerning A, which are separately the restricted isometry property (RIP) [3] and the mutual coherence determined as [10, 12]

$$\mu = \max_{1\le i<j\le N} |\langle A_i, A_j\rangle|. \tag{1.2}$$

For a more general definition of coherence, i.e. the block-coherence, see [13].

It is well known that ℓ_1 minimization method [7], viewed as a convex extension of ℓ_0 minimization method, presents an efficient approach for recovering s-sparse signal in numerous contexts. The ℓ_0 minimization method and the ℓ_1 minimization method are respectively

$$\begin{aligned} &\min_{\tilde{x}\in\mathbb{R}^N} \|\tilde{x}\|_0 \\ &\text{s.t.} \quad y = A\tilde{x} + z, \quad \|z\|_2 \le \epsilon, \\ &\min_{\tilde{x}\in\mathbb{R}^N} \|\tilde{x}\|_1 \\ &\text{s.t.} \quad y = A\tilde{x} + z, \quad \|z\|_2 \le \epsilon. \end{aligned}$$

Here $\|\tilde{x}\|_0$ represents the number of non-zero coordinates in $\tilde{x}$. In recent years, one alternative approach of estimating the s-sparse signal in the references [6, 11, 14, 24, 25, 29] is to solve the following ℓ_r minimization model:

$$\begin{aligned} &\min_{\tilde{x}\in\mathbb{R}^N} \|\tilde{x}\|_r^r \\ &\text{s.t.} \quad y = A\tilde{x} + z, \quad \|z\|_2 \le \epsilon, \end{aligned} \tag{1.3}$$

where $\|\tilde{x}\|_r^r = \sum_{i=1}^N |\tilde{x}_i|^r$ with $\tilde{x}_i$ being the i-th entry of $\tilde{x}, r \in (0, 1]$ and

$$\|z\|_2 = \left(\sum_{i=1}^m z_i^2\right)^{\frac{1}{2}}.$$

Compared with ℓ_1 minimization, although it is more difficult to resolve model (1.3) because of its noncovexity, there still exist a lot of algorithms to find the local optimal solution of (1.3).

Besides, it has been showed by [5] that solving the ℓ_r minimization model with small r can significantly reduce the number of measurements.

Zhou and Yu [31] recently introduced a novel weighted $\ell_r - \ell_1$ minimization method as follows:

$$\begin{aligned} &\min_{\tilde{x}\in\mathbb{R}^N} \|\tilde{x}\|_r^r - \alpha\|\tilde{x}\|_1^r \\ &\text{s.t.} \quad y = A\tilde{x} + z, \quad \|z\|_2 \le \epsilon, \end{aligned} \tag{1.4}$$

where $\alpha \in [0,1], 0 < r \le 1, \|\tilde{x}\|_1 = \sum_{i=1}^N |\tilde{x}_i|$, and suppose that $\alpha \ne 1$ in the case of $r = 1$. It is obvious that (1.4) degenerates to the traditional ℓ_r minimization model in the case of $\alpha = 0$. Though resolving model (1.4) is harder than resolving model (1.3) for mixed norm in it, a great number of algorithms also can be employed to solve it, see, e.g. [28, 30, 31]. Furthermore, it can enhance the ℓ_1 minimization in a robust pattern. Because there are effective algorithms for resolving (1.4), main objective of this paper is to exploit a sufficient condition that can guarantee the stable recovery of x through resolving (1.4) rather than discussing how to efficiently resolving (1.4).

Recently, many literatures [2,28,31] have studied the sufficient conditions for robust recovery of x via solving model (1.4) based on RIP. Different from former contributions utilizing the RIP to depict the sufficient condition, this paper makes use of the mutual coherence μ to describe a new sufficient condition. Actually, under the same conditions, the mutual coherence μ of a given matrix is easier to calculate than its RIP constant. In addition, it is difficult to verify the RIP condition within efficient time for a given matrix.

Since the Dantzig selector noise is also extensively investigated noise in compressed sensing, the sufficient condition of stably reconstruction x through

$$\begin{aligned} &\min_{\tilde{x}\in\mathbb{R}^N} \|\tilde{x}\|_r^r - \alpha\|\tilde{x}\|_1^r \\ &\text{s.t.} \quad y = A\tilde{x} + z, \quad \|A^\top z\|_\infty \le \epsilon \end{aligned} \tag{1.5}$$

is also discussed.

Our results show that any s-sparse signal x from (1.1) can be robustly reconstructed through settling (1.4) or (1.5) provided that the mutual coherence μ of A fulfills $\mu < \kappa(s; r, \alpha, N)$ for $s > 1$ and $\alpha^{1/r} N^{1/2} < 1$. To our best of knowledge, this is the first sufficient condition for robust reconstruction of x by solving (1.4) and (1.5) based on mutual coherence. The Gaussian noise is of special interest in signal and image processing as well as in statistics. Since the Gaussian noise is essentially bounded, the results can be generalized to it.

This paper is constructed as follows. We begin by providing notations and lemmas that will be needed in our analysis in Section 2. The main results and its corresponding proofs are presented in Section 3. Numerical simulations are conducted in Section 4 to contrast the effectuality of (1.4) and (1.5) with those of (1.3) and its associating Dantzig selector noise case. We prove the lemmas in Section 5. In Section 6, a conclusion is provided.

2. Preliminaries

We first explicate some necessary notations. Let S represent the support of x, that is, $S = \{i \in [N] \,|\, x_i \ne 0\}$. For any set T, let x_T stand for a vector that keeps the entries indexed by T of x and 0 otherwise. Let S^c indicate the complement of S, that is, $S^c = \{1, 2, \ldots, N\} \backslash S$. For any matrix $\Phi, \Phi^\top$ denote the transpose of Φ.

The concept of s-th r-restricted isometry constant proposed by Chartrand and Staneva [6] is as follows.

Definition 2.1 ([6, 31]). *For $0 < r \leq 1$ and $s > 0$, one defines the s-th r-restricted isometry constant of a matrix $A \in \mathbb{R}^{m\times N}$ to be the smallest number which fulfills*

$$(1-\delta_s)\|u\|_2^r \leq \|Au\|_r^r \leq (1+\delta_s)\|u\|_2^r \tag{2.1}$$

for any s-sparse vector $u \in \mathbb{R}^N$.

In what follows, we present some auxiliary lemmas that are needed for the proofs of our main results.

Lemma 2.1 ([1, 20, 26]). *For any s-sparse vector u, we get*

$$1-(s-1)\mu \leq \frac{\|Au\|_2^2}{\|u\|_2^2} \leq 1+(s-1)\mu. \tag{2.2}$$

Lemma 2.2. *For a general vector x (i.e. x is not s-sparse), we have*

$$\|h_{S^c}\|_r^r \leq \|h_S\|_r^r + \alpha\|h\|_1^r + 2\|x_{S^c}\|_r^r. \tag{2.3}$$

Lemma 2.3. *Let $\hat{x}$ be the minimizer of (1.4), and stand for the recovery error $h = \hat{x} - x$. It is assumed that A and z in (1.1) fulfill*

$$\mu < \frac{1}{s-1+2^{\frac{1}{r}-1}s^{\frac{1}{r}}}, \tag{2.4}$$

and $\|z\|_2 \leq \epsilon$, separately. Then,

$$\|h_S\|_2 \leq \frac{2\epsilon\sqrt{1+(s-1)\mu}}{1-\left(s-1+2^{\frac{1}{r}-1}s^{\frac{1}{r}}\right)\mu} + \frac{2^{\frac{1}{r}-1}\mu N^{\frac{1}{2}}\alpha^{\frac{1}{r}}s^{\frac{1}{2}}\|h\|_2}{1-\left(s-1+2^{\frac{1}{r}-1}s^{\frac{1}{r}}\right)\mu}. \tag{2.5}$$

Lemma 2.4. *Let $\hat{x}$ be the minimizer of (1.5), and indicate the recovery error $h = \hat{x} - x$. We assume A and z in (1.1) meet (2.4) and $\|A^\top z\|_\infty \leq \epsilon$, respectively. Then,*

$$\|h_S\|_2 \leq \frac{2\epsilon\sqrt{s}}{1-\left(s-1+2^{\frac{1}{r}-1}s^{\frac{1}{r}}\right)\mu} + \frac{2^{\frac{1}{r}-1}\mu N^{\frac{1}{2}}\alpha^{\frac{1}{r}}s^{\frac{1}{2}}\|h\|_2}{1-\left(s-1+2^{\frac{1}{r}-1}s^{\frac{1}{r}}\right)\mu}. \tag{2.6}$$

3. Main Results

In this part, based on the mutual coherence of A, the sufficient conditions for robust reconstruction of s-sparse signals x via (1.4) and (1.5) are explored. First of all, a sufficient condition for robust reconstruction of s-sparse signals x by (1.4) is given, which is stated as follows.

Theorem 3.1. *Let $\hat{x}$ be the solution of (1.4). If A and z in (1.1) fulfill*

$$\begin{aligned}\mu < &\left[\left(s-1+2^{\frac{1}{r}-1}s^{\frac{1}{r}}\right)^2 - 2^{\frac{2}{r}-2}\alpha^{\frac{2}{r}}N\right]^{-1} \\ &\times\left\{s-1+2^{\frac{1}{r}-1}s^{\frac{1}{r}} + 2^{\frac{2}{r}-3}\alpha^{\frac{2}{r}}N - \sqrt{2^{\frac{2}{r}-2}\alpha^{\frac{2}{r}}N(s+2^{\frac{1}{r}-1}s^{\frac{1}{r}}) + 2^{\frac{4}{r}-6}\alpha^{\frac{4}{r}}N^2}\right\} \\ =:&\ \kappa(s;r,\alpha,N),\end{aligned} \tag{3.1}$$

and $\|z\|_2 \leq \epsilon$ *for* $s > 1$ *and* $\alpha^{1/r} N^{1/2} < 1$, *then*

$$\|\hat{x} - x\|_2 \leq C\epsilon, \tag{3.2}$$

where C *depends on* μ, r, N, α *and* s, *which is determined in* (5.22).

Then, a sufficient condition for robust recovery of s-sparse signal x by (1.5) is provided.

Theorem 3.2. *Let* $\hat{x}$ *be the minimizer of* (1.5). *If* A *and* z *in* (1.1) *fulfill* (3.1) *and* $\|A^\top z\|_\infty \leq \epsilon$ *for* $s > 1$ *and* $\alpha^{1/r} N^{1/2} < 1$, *then*

$$\|\hat{x} - x\|_2 \leq D\epsilon, \tag{3.3}$$

where D *relies on* μ, r, N, α *and* s, *which is defined in* (5.28).

Remark 3.1. From Theorems 3.1 and 3.2, we can observe that any s-sparse signal x corrupted by the bounded ℓ_2 noise or Dantzig selector noise can be robustly reconstructed through (1.4) and (1.5), separately, if the matrix A satisfies condition (3.1), and the associating reconstruction error can be controlled by (3.2) and (3.3), separately. This reveals the effectiveness of reconstructing s-sparse signals by methods (1.4) and (1.5) from a theoretical point of view.

Remark 3.2. For the model degradation, when $r = 1$ and $\alpha \neq 1$, the mutual coherence condition (2.4) is the same as [1, Theorems 2.1, 2.2].

Remark 3.3. We now study the error bound of Theorem 3.1 and the literature [31]. The curves of the error bound noise constant (i.e. C) of Theorem 3.1 and the literature [31] with respect to the parameter r are given in Fig. 3.1. Observation of the figure shows that our established error bound noise constant is smaller than that of the literature [31] when r takes values between 0.4 and 0.6.

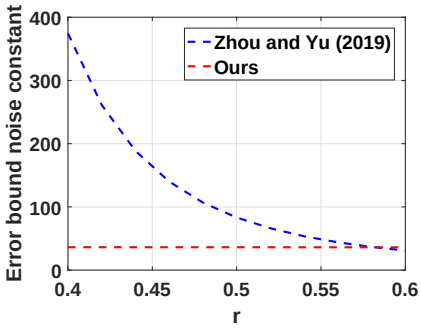

Fig. 3.1. Comparison error bound noise constant.

Remark 3.4. The literature has presented the relationship between RIP and mutual coherence. It follows from [18] that $\delta_s \leq (s-1)\mu$. Moreover, the monotone property on δ_s can be found in [16, 17]: $\delta_s \leq \delta_t$, if $s \leq t \leq N$. With the above connections, the results regarding RIP in literature can also be characterized with respect to mutual coherence. Recently, Zhou [30] provided the RIP-based exploration result for the non-convex weighted $\ell_r - \ell_1$ minimization issue (1.4). He evidenced that if the measurement matrix A meets $\delta_{2s} < \tau/\sqrt{\tau^2 + \gamma}$ for $s \geq 2$ with

$$\tau = \left(\frac{s - \alpha s^r}{s + \alpha s^r}\right)^{\frac{1}{r}}, \quad \gamma = \frac{2^{\frac{2}{r}-2}}{s}\left[(1 + \alpha - \alpha 2^r)^{-\frac{2}{r}}(s+1) + 1\right],$$

then a stable and robust reconstruction can be ensured for any (nearly) sparse signal through the weighted $\ell_r - \ell_1$ minimization approach. Utilizing the above relationship, the corresponding coherence condition is

$$\mu < \frac{\tau}{(2s-1)\sqrt{\tau^2+\gamma}}. \tag{3.4}$$

In Fig. 3.2, we give upper bounds for the coherence conditions of (3.1) and (3.4). Images of the variation of coherence with r are plotted in Fig. 3.2(a), where $\alpha = 0.9, N = 64, s = 0.5$. Fig. 3.2(b) plots the curve between coherence and the parameter α, where $r = 0.7$. In Fig. 3.2(c), the curve between coherence and sparsity s is depicted, where $r = 0.9, \alpha = 0.9$. Observing the figure, we can know that when $r \in (0.55, 1), \alpha \in (0.3, 1), s \in (15, 256)$, condition that we obtain is weaker than that of Zhou [30].

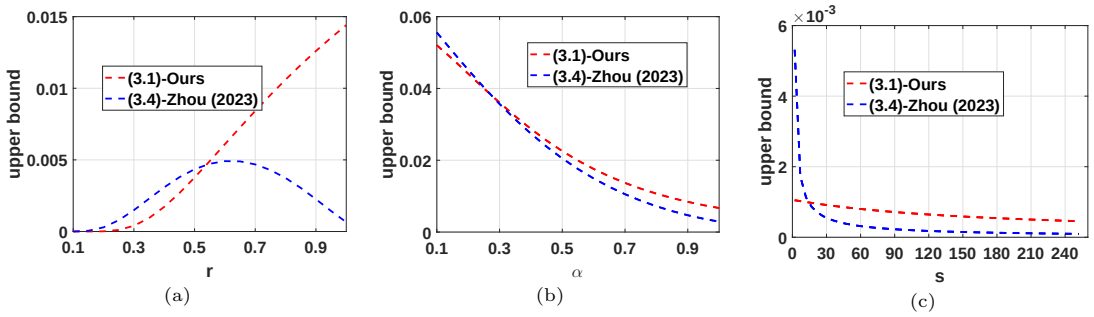

(a) (b) (c)

Fig. 3.2. Comparison coherence conditions (3.4) and (3.1).

4. Numerical Experiments

To testify the validity of the model and our obtained coherence theory, we first conduct an experiment on the construction of the measurement matrix, followed by some comparative experiments of models. In the experiment, the length of the vector and the number of samples are fixed as $N = 256$ and $m = 128$, separately.

4.1. Measurement matrix construction

In accordance with the obtained Theorems 3.1 and 3.2, the method (1.4) or (1.5) will carry out robustness provided that the measurement matrix A fulfills the assumption (3.1). Instinctively, when those matrices whose mutual coherence is smaller than its upper bound $\kappa(s; r, \alpha, N)$ (for known s) are chosen, this assumption will be satisfied without difficulty. Furthermore, Welch [23] also showed that the mutual coherence of all matrices A is contained by a lower boundary that is at present said to be the Welch bound defined as

$$\mu(A) \geq \sqrt{\frac{N-m}{m(N-1)}}. \tag{4.1}$$

Hence, it is natural for us to devise the measurement matrix whose mutual coherence can achieve the Welch bound. Until now a variety of approaches are capable of being utilized to produce these matrices, and we refer readers to [21, 22, 27]. The article utilizes the alternating projection (AP) approach to produce the wanted measurement matrices which have small coherence introduced by Tropp *et al.* [19]. In order to verify the capability of this AP approach,

we have conducted experiments on Gaussian, Bernoulli and partial Fourier random matrices, respectively. Figs. 4.1(a)-(c) respectively give the coherence comparisons of these three types of matrices before and after processing using the AP method, where $d_i, i \in \{1, 2, \ldots, m\}$, stands for the i-th column of the matrix. It is not difficult to find that the coherence for these three types of matrices processed by the AP method is very close to the Welch lower bound. In the subsequent experiments, we will use the AP method to produce the wanted measurement matrix based on coherence and choose the Gaussian random matrix as the matrix to be processed by the AP method.

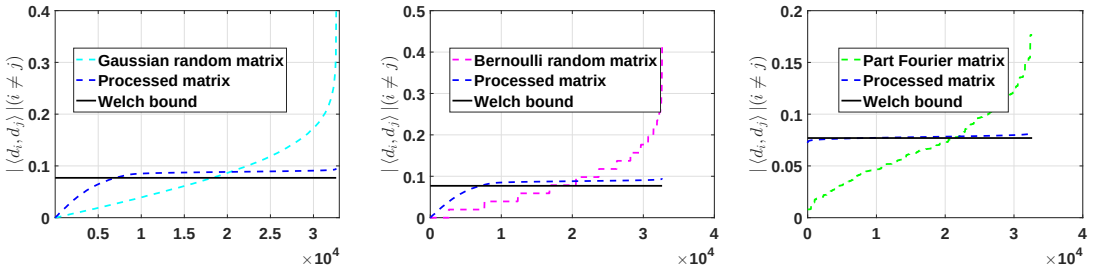

(a) Gaussian random matrix (b) Bernoulli random matrix (c) Partial Fourier random matrix

Fig. 4.1. Coherence comparisons.

4.2. Model comparison

To solve the issue (1.4), it is first transformed into the below unrestricted form

$$\min_{\tilde{x}\in\mathbb{R}^N} \lambda\big(\|\tilde{x}\|_r^r - \alpha\|\tilde{x}\|_1^r\big) + \frac{1}{2}\|y - A\tilde{x}\|_2^2, \tag{4.2}$$

where λ denotes the regularization parameter with $\lambda > 0$. Zhou and Yu [31] pointed out that the issue can be settled via combining an iteratively reweighted least square (IRLS) approach and a difference for convex functions method (DCA). In the external circle, one can employ the IRLS to approach the item $\|\tilde{x}\|_r^r$, and take advantage of a reweighted 1 norm of iterative to close in $\|\tilde{x}\|_1^r$, that is,

$$\tilde{x}^{k+1} = \arg\min_{\tilde{x}\in\mathbb{R}^N} \lambda\|W^k\tilde{x}\|_2^2 - \alpha\lambda\nu^k\|\tilde{x}\|_1 + \frac{1}{2}\|y - A\tilde{x}\|_2^2, \tag{4.3}$$

where

$$W^k = \mathrm{diag}\Big\{\big((x_i^k)^2 + \varepsilon_k\big)^{\frac{r}{4}-\frac{1}{2}}\Big\}, \quad \nu^k = \|\tilde{x}^k\|_1^{r-1}.$$

For the inner loop adopted to address (4.3), it can be regarded as a discrepancy minimization issue for a pair of convex functions, namely, goal function

$$I(x) = \left(\frac{1}{2}\|y - A\tilde{x}\|_2^2 + \lambda\|W^k\tilde{x}\|_2^2\right) - \alpha\lambda\nu^k\|\tilde{x}\|_1 =: J(\tilde{x}) - L(\tilde{x}).$$

$L(\tilde{x})$ is linearized as $L(\tilde{x}^{k+1,n}) + \langle y^{k+1,n}, \tilde{x} - \tilde{x}^{k+1,n}\rangle$ with $y^{k+1,n} \in \partial L(\tilde{x}^{k+1,n})$ and replace $L(x)$ with its approximation. Therefore,

$$\tilde{x}^{k+1,n+1} = \arg\min_{\tilde{x}\in\mathbb{R}^N} \frac{1}{2}\|y - A\tilde{x}\|_2^2 + \lambda\|W^k\tilde{x}\|_2^2$$

$$
\begin{aligned}
&- \big(\alpha\lambda\nu^k\|\tilde{x}^{k+1,n}\|_1 + \langle\alpha\lambda\nu^k\mathrm{sign}(\tilde{x}^{k+1,n}), \tilde{x}-\tilde{x}^{k+1,n}\rangle\big)\\
&= \arg\min_{\tilde{x}\in\mathbb{R}^N} \frac{1}{2}\|y - A\tilde{x}\|_2^2 + \lambda\|W^k\tilde{x}\|_2^2 - \langle\alpha\lambda\nu^k\mathrm{sign}(\tilde{x}^{k+1,n}), \tilde{x}\rangle\\
&= \big(A^\top A + 2\lambda(W^k)^\top W^k\big)^{-1}\big(A^\top y + \alpha\lambda\nu^k\mathrm{sign}(\tilde{x}^{k+1,n})\big) \qquad (4.4)
\end{aligned}
$$

with $\mathrm{sign}(\cdot)$ represents the sign function.

4.2.1. Experiments on random synthetic data

First, we consider choosing an appropriate regularization parameter λ. Without loss of generality, the signal with sparsity $s = 25$ is taken as the test signal, and Fig. 4.2 demonstrates the specific results from experiments. Here, we fix $\alpha = 0.2$. As can be seen from the figure, it is more appropriate to choose $\lambda = 1 \times 10^{-3}$.

In the following experiments, the reconstruction capability of the weighted $\ell_r - \ell_1$ minimization approach (1.4) is compared with that of the ℓ_r minimization approach (1.3). Additionally, unless specified, we take $r = 0.5$ and $\alpha = 1$. First of all, we conduct experiments on randomly generated data. Under different noise scenarios, the signal to noise ratio (SNR) of two methods varies with the sparsity s as indicated in Fig. 4.3, where SNR$= 20\log(\|x\|_2/\|\hat{x} - x\|_2)$. Observing the figure, we can see that the weighted $\ell_r - \ell_1$ minimization method performs better than the ℓ_r minimization method.

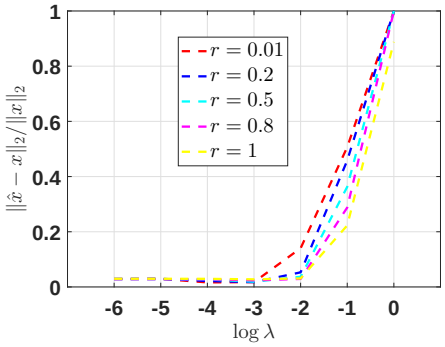

Fig. 4.2. Choice of regularization parameter λ.

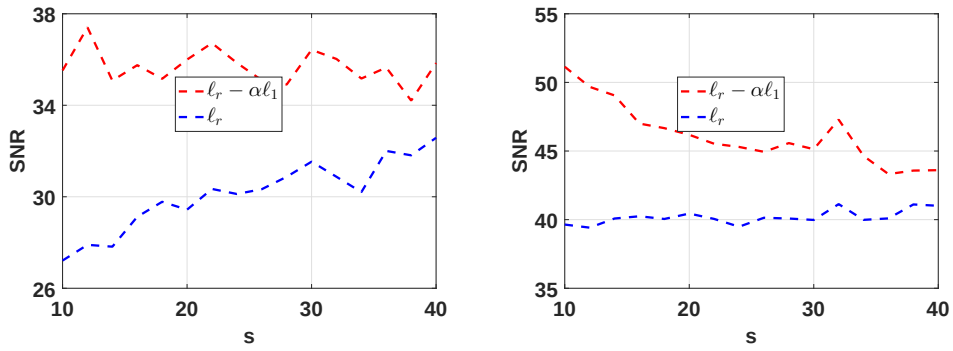

(a) ℓ_2 bounded noise (b) Dantzig selector noise

Fig. 4.3. Recovery performance of two algorithms.

4.2.2. Experiments on grey image recovery

In this subsection, we will apply the model (1.4) as well as the model (1.3) to the topic of grey image reconstruction. To appraise the quality of the reconstructed pictures, the peak signal-to-noise ratio (PSNR) and the structural similarity (SSIM) targets are employed. For SSIM target, we refer readers to [22]. The PSNR target is defined by

$$\mathrm{PSNR} = 10\log_{10}\frac{255^2 \times m \times N}{\|X - \tilde{X}\|_F^2},$$

where X represents the primitive picture with size $m \times N$ and $\tilde{X}$ indicates the reconstructed picture with size $m \times N$.

Before comparing the model performance, we necessarily choose an appropriate regularization parameter λ since it is significant in the algorithm on (1.4). For this purpose, the associating algorithm of (1.4) is utilized to the reconstruction of classical Lena picture (displayed in Fig. 4.7(a)) under different values of λ. The relationship between λ and the PSNR and SSIM results is drawn in Fig. 4.4. It is recommended to take $\lambda = 10^{-4}$. The curves for model (1.4) between PSNR and SSIM in relation to parameters r and α in different values of α and r, respectively, are depicted in Figs. 4.5 and 4.6. Looking at the images it is clear that the choice of $r = 0.2, 0.6, \alpha = 0.1, 0.2, 0.4, 0.5, 0.8$ or $r = 0.5, \alpha = 0.1, 0.2, 0.4$ or $r = 1.0, \alpha = 0.1, 0.2$ is appropriate. In the following, put $\lambda = 10^{-4}$. The reconstruction capability of the Lena picture and one of its part is drawn in Fig. 4.7 and Fig. 4.8. Observe that the reconstruction proceeding is not conducted first-hand regarding the entire Lena picture, but concerning its little non-intersecting parts. Specifically, the former Lena picture is first partitioned into 256

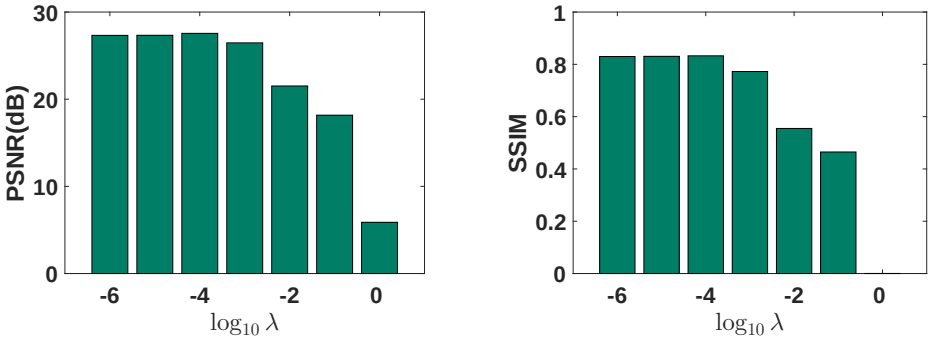

Fig. 4.4. PSNR and SSIM performance of algorithm of (1.4) under different λ.

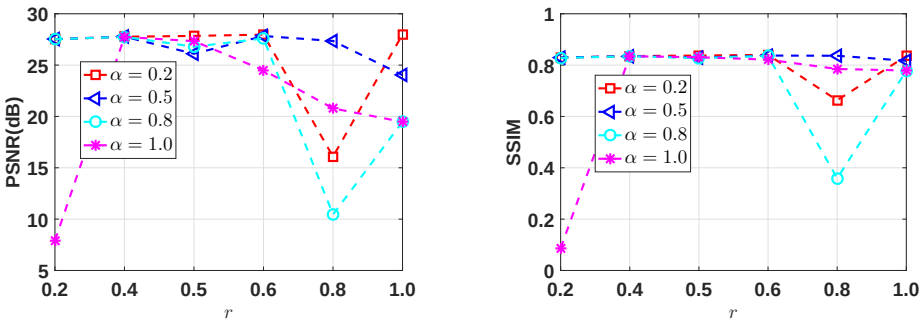

Fig. 4.5. PSNR and SSIM performance of algorithm of (1.4) under different r.

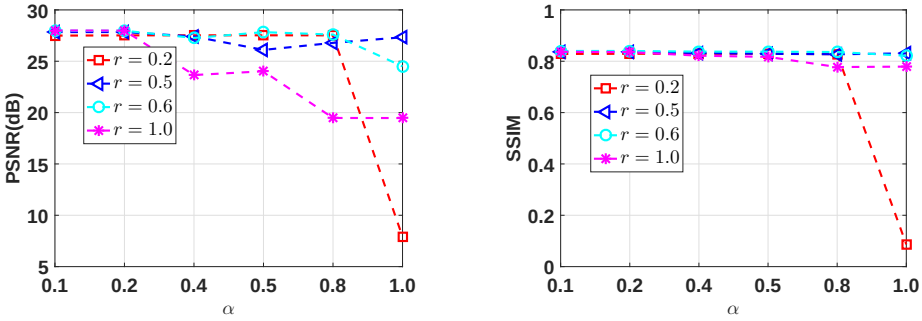

Fig. 4.6. PSNR and SSIM performance of algorithm of (1.4) under different α.

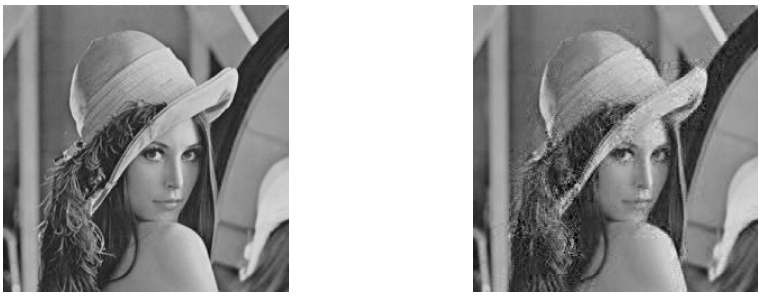

(a) Lena picture (256 × 256)

(b) Reconstructed Lena picture

Fig. 4.7. Reconstruction of Lena picture with $r = 0.6$ and $\alpha = 0.2$. In (b), the derived PSNR and SSIM results are separately 27.97 dB and 0.840.

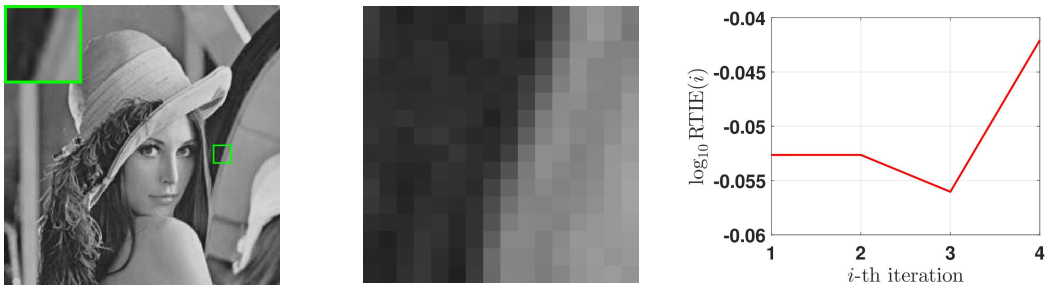

(a) A part Lena picture [21]

(b) Reconstructed part

(c) Convergence on the part displayed in Fig. 4.8(a)

Fig. 4.8. Convergence outcome for algorithm with $r = 0.6$ and $\alpha = 0.2$. In (b), the gained PSNR outcome is 35.31dB and SSIM outcome is 0.98. In (c), the relative true iteration error is abbreviated as RTIE, i.e. $\mathrm{RTIE}(i) = \|x^{k+1} - x\|_2/\|x\|_2$ with x standing for the original signal.

non-intersecting parts, each having dimension 16×16, and afterwards reconstruct these little parts individually. Observe that these small parts are not sparse themselves, but sparse in terms of some base such as wavelet transform or discrete cosine transform or Fourier transform. In the present article, the MATLAB command `dct2` is utilized for producing the wanted sparse base and hereafter reconstruct the caused sparse moduli from their a small amount of measurements. In the above image reconstruction experiments, the number of samples is usually fixed as $m = 102$. Actually, it can be seen from Fig. 4.9 that the PSNR/SSIM is gradually getting better as the number of samples increases.

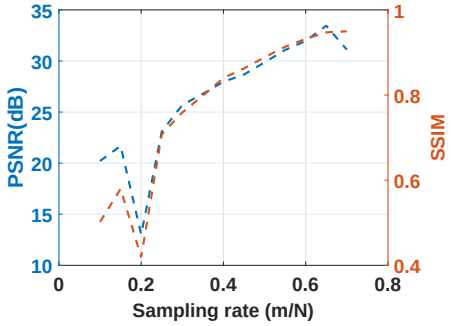

Fig. 4.9. PSNR|SSIM results of the Lena picture reconstructed by (1.4) under different sampling ratios.

Fig. 4.10. The test pictures with size 256×256. We number them sequentially from 1 to 20, from left to right, and from upper apex to base.

With the above preparatory work, we now make use of the models (1.4) and (1.3) to the reconstruction of additional greys pictures. The 20 commonly used test images, each of size 256×256, are given in Fig. 4.10, and the PSNR/SSIM results obtained by the two models for the test images are given in Table 4.1. It is easily observed that model (1.4) carries out better than model (1.3).

4.2.3. Experiments on FECG signals

Next, we carry out algorithm comparison experiments on real FECG signals exhibited in Fig. 4.11. It can be seen from Table 4.2 that for most real FECG signals, the weighted $\ell_{0.6} - 0.2\ell_1$ minimization approach exercises better than the $\ell_{0.6}$ minimization method with respect to signal-to-noise ratio.

Table 4.1: PSNR|SSIM results of 20 pictures by different models.

	1	2	3	4	5
$\ell_{0.6}-0.2\ell_1$	**32.02|0.922**	**25.67|0.769**	**27.99|0.832**	**22.76|0.638**	**26.19|0.783**
$\ell_{0.6}$	31.21|0.898	24.91|0.730	27.30|0.802	22.11|0.600	25.45|0.742
	6	7	8	9	10
$\ell_{0.6}-0.2\ell_1$	**28.26|0.827**	**25.49|0.813**	**23.82|0.769**	**21.95|0.705**	**28.88|0.782**
$\ell_{0.6}$	27.50|0.791	24.84|0.779	23.11|0.745	21.14|0.665	28.24|0.748
	11	12	13	14	15
$\ell_{0.6}-0.2\ell_1$	**27.96|0.796**	**31.54|0.875**	**23.51|0.679**	**27.35|0.752**	**26.66|0.724**
$\ell_{0.6}$	27.38|0.763	30.45|0.836	22.92|0.644	26.50|0.712	26.01|0.689
	16	17	18	19	20
$\ell_{0.6}-0.2\ell_1$	**23.91|0.737**	**24.40|0.703**	**27.09|0.815**	**28.25|0.837**	**24.44|0.742**
$\ell_{0.6}$	23.21|0.701	23.64|0.663	26.33|0.783	26.98|0.799	23.51|0.702

Table 4.2: SNR results by two methods.

	a	b	c	d	e	f	g	h
$\ell_{0.6}-0.2\ell_1$	**5.071**	**6.095**	**5.649**	**1.655**	**6.351**	5.591	3.031	3.23
$\ell_{0.6}$	3.539	4.87	3.869	-0.3962	4.424	5.854	5.499	6.87

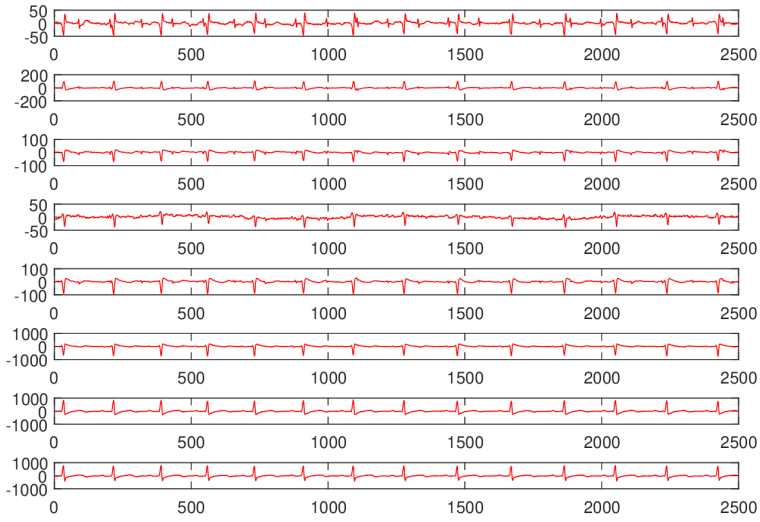

Fig. 4.11. All FECG signals. These signals are numbered a through h from top to bottom.

5. Proofs

In this section, we prove the main results. First, we give the proofs of previous lemmas.

Proof of Lemma 2.2. Here we assume that x is a general signal. Since $\hat{x}$ is the optimal solution of (1.4) or (1.5), it implies that

$$\|x\|_r^r - \alpha\|x\|_1^r \geq \|\hat{x}\|_r^r - \alpha\|\hat{x}\|_1^r.$$

Due to $h = \hat{x} - x$, we get

$$\|x_S\|_r^r + \|x_{S^c}\|_r^r - \alpha\|x\|_1^r \geq \|x_S + x_{S^c} + h_S + h_{S^c}\|_r^r - \alpha\|x + h\|_1^r. \tag{5.1}$$

By using the triangular inequality and the inequality $(a+b)^r \leq a^r + b^r$ for nonnegative a and b, we get

$$\begin{aligned}
&\|x_S + x_{S^c} + h_S + h_{S^c}\|_r^r - \alpha\|x + h\|_1^r \\
&\geq \|x_S + h_S\|_r^r + \|x_{S^c} + h_{S^c}\|_r^r - \alpha(\|x\|_1 + \|h\|_1)^r \\
&\geq \|x_S\|_r^r - \|h_S\|_r^r + \|h_{S^c}\|_r^r - \|x_{S^c}\|_r^r - \alpha\|x\|_1^r - \alpha\|h\|_1^r.
\end{aligned} \tag{5.2}$$

A combination of (5.1) and (5.2) leads to the desired result. □

Proof of Lemma 2.3. Note that $\hat{x}$ is a minimizer of (1.4) and z fulfills $\|z\|_2 \leq \epsilon$, by the equality $h = \hat{x} - x$ and the triangular inequality, then

$$\|Ah\|_2 = \|A(\hat{x} - x)\|_2 \leq \|A\hat{x} - y\|_2 + \|Ax - y\|_2 \leq 2\epsilon. \tag{5.3}$$

Combining with Lemma 2.1, (5.3) and the inequality $|\langle u, v\rangle| \leq \|u\|_2\|v\|_2$ for $0 \neq u, v \in \mathbb{R}^m$, we get

$$|\langle Ah, Ah_S\rangle| \leq \|Ah\|_2\|Ah_S\|_2 \leq 2\epsilon\sqrt{1 + (s-1)\mu}\,\|h_S\|_2. \tag{5.4}$$

By applying (1.2), it results in

$$|A_i^\top A_j| \leq \mu, \quad 1 \leq i < j \leq N, \tag{5.5}$$

which implies that

$$\begin{aligned}
&|\langle Ah_S, Ah_{S^c}\rangle| = \left|\left\langle \sum_{i\in S} A_i h_i, \sum_{j\in S^c} A_j h_j, \right\rangle\right| \\
&\leq \sum_{i\in S}\sum_{j\in S^c} |\langle A_i, A_j\rangle|\,|h_i|\,|h_j| \leq \mu\left(\sum_{i\in S}|h_i|\right)\left(\sum_{j\in S^c}|h_j|\right) \\
&= \mu\|h_S\|_1\|h_{S^c}\|_1 \leq \mu s^{\frac{1}{2}}\|h_S\|_2\|h_{S^c}\|_r \\
&\overset{(a)}{\leq} \mu s^{\frac{1}{2}}\|h_S\|_2\big(\|h_S\|_r^r + \alpha\|h\|_1^r\big)^{\frac{1}{r}} \\
&\overset{(b)}{\leq} 2^{\frac{1}{r}-1}\mu s^{\frac{1}{2}}\|h_S\|_2\left(\|h_S\|_r + \alpha^{\frac{1}{r}}\|h\|_1\right) \\
&\overset{(c)}{\leq} 2^{\frac{1}{r}-1}\mu s^{\frac{1}{2}}\|h_S\|_2\left(s^{\frac{1}{r}-\frac{1}{2}}\|h_S\|_2 + \alpha^{\frac{1}{r}}N^{\frac{1}{2}}\|h\|_2\right) \\
&= 2^{\frac{1}{r}-1}\mu s^{\frac{1}{r}}\|h_S\|_2^2 + 2^{\frac{1}{r}-1}\mu N^{\frac{1}{2}}\alpha^{\frac{1}{r}}s^{\frac{1}{2}}\|h_S\|_2\|h\|_2,
\end{aligned} \tag{5.6}$$

where (a) follows from Lemma 2.2, (b) is due to $(a^r + b^r)^{1/r} \leq 2^{1/r-1}(a+b)$ for any $a, b \geq 0$, and (c) is because of the Hölder's inequality and the Cauchy-Schwarz inequality. By using Lemma 2.1 together with the triangular inequality, it leads to

$$\begin{aligned}
|\langle Ah, Ah_S\rangle| &= |\langle Ah_S + Ah_{S^c}, Ah_S\rangle| \geq |\langle Ah_S, Ah_S\rangle| - |\langle Ah_{S^c}, Ah_S\rangle| \\
&\geq [1 - (s-1)\mu]\,\|h_S\|_2^2 - |\langle Ah_{S^c}, Ah_S\rangle|.
\end{aligned}$$

Plugging (5.6) into the above inequality, we get

$$|\langle Ah, Ah_S\rangle| \geq \left[1 - (s - 1 + 2^{\frac{1}{r}-1}s^{\frac{1}{r}})\mu\right] \|h_S\|_2^2 - 2^{\frac{1}{r}-1}\mu N^{\frac{1}{2}}\alpha^{\frac{1}{r}}s^{\frac{1}{2}}\|h_S\|_2\|h\|_2. \tag{5.7}$$

Combining with (2.4), (5.4) and (5.7), the wanted result follows. □

Proof of Lemma 2.4. For $\hat{x}$ is a minimizer of (1.5) and z fulfills $\|A^\top z\|_\infty \leq \epsilon$, by $h = \hat{x} - x$ and the triangular inequality, we have

$$\|A^\top Ah\|_\infty \leq \|A^\top A(\hat{x} - x)\|_\infty \leq \|A^\top(A\hat{x} - y)\|_\infty + \|A^\top(Ax - y)\|_\infty \leq 2\epsilon. \tag{5.8}$$

By applying Hölder inequality, it implies that

$$|\langle Ah, Ah_S\rangle| \leq |\langle A^\top Ah, h_S\rangle| \leq \|h_S\|_1\|A^\top Ah\|_\infty \leq s^{\frac{1}{2}}\|h_S\|_2\|A^\top Ah\|_\infty.$$

Putting (5.8) into the above inequality, we get

$$|\langle Ah, Ah_S\rangle| \leq 2\epsilon s^{\frac{1}{2}}\|h_S\|_2. \tag{5.9}$$

A combination of (5.7) and (5.9), we obtain the desired result. □

Proof of Theorem 3.1. Observing that $\|A_i\|_2 = 1, i = 1, 2, \ldots, N$, and (1.2), it leads to

$$\begin{aligned}
\langle Ah, Ah\rangle &= \sum_{i=1}^N\sum_{j=1}^N\langle A_ih_i, A_jh_j\rangle = \sum_{i=1}^N\langle A_ih_i, A_ih_i\rangle + \sum_{i=1}^N\sum_{j=1,j\neq i}^N\langle A_ih_i, A_jh_j\rangle \\
&= \sum_{i=1}^N\|A_i\|_2^2|h_i|^2 + \sum_{i=1}^N\sum_{j=1,j\neq i}^N\langle A_i, A_j\rangle h_ih_j \\
&\geq \sum_{i=1}^N|h_i|^2 - \mu\sum_{i=1}^N\sum_{j=1,j\neq i}^N|h_ih_j| = \|h\|_2^2 - \mu\left(\sum_{i=1}^N\sum_{j=1}^N|h_ih_j| - \sum_{i=1}^N|h_i|^2\right) \\
&= (1+\mu)\|h\|_2^2 - \mu\|h\|_1^2 = (1+\mu)\|h\|_2^2 - \mu(\|h_S\|_1 + \|h_{S^c}\|_1)^2 \\
&\geq (1+\mu)\|h\|_2^2 - \mu(\|h_S\|_1 + \|h_{S^c}\|_r)^2 \\
&\overset{(a)}{\geq} (1+\mu)\|h\|_2^2 - \mu\left[\|h_S\|_1 + \left(\|h_S\|_r^r + \alpha\|h\|_1^r\right)^{\frac{1}{r}}\right]^2 \\
&\overset{(b)}{\geq} (1+\mu)\|h\|_2^2 - \mu\left[s^{\frac{1}{2}}\|h_S\|_2 + 2^{\frac{1}{r}-1}\left(\|h_S\|_r + \alpha^{\frac{1}{r}}\|h\|_1\right)\right]^2 \\
&\overset{(c)}{\geq} (1+\mu)\|h\|_2^2 - \mu\left[s^{\frac{1}{2}}\|h_S\|_2 + 2^{\frac{1}{r}-1}\left(s^{\frac{1}{r}-\frac{1}{2}}\|h_S\|_2 + \alpha^{\frac{1}{r}}N^{\frac{1}{2}}\|h\|_2\right)\right]^2 \\
&= (1+\mu)\|h\|_2^2 - \mu\left[\left(s^{\frac{1}{2}} + 2^{\frac{1}{r}-1}s^{\frac{1}{r}-\frac{1}{2}}\right)\|h_S\|_2 + 2^{\frac{1}{r}-1}\alpha^{\frac{1}{r}}N^{\frac{1}{2}}\|h\|_2\right]^2,
\end{aligned} \tag{5.10}$$

where (a) follows from (2.3), (b) is because of the Cauchy-Schwarz inequality and $(a^r + b^r)^{1/r} \leq 2^{1/r-1}(a+b)$ for any $a, b \geq 0$, and (c) is thanks to the Hölder inequality.

Set

$$1 - \left(s - 1 + 2^{\frac{1}{r}-1}s^{\frac{1}{r}}\right)\mu =: p, \quad s[1 + (s-1)\mu] =: q, \quad \left(1 + 2^{\frac{1}{r}-1}s^{\frac{1}{r}-1}\right)^2 q = \hat{q}.$$

By (2.5), (5.3) and (5.10), it implies that

$$
\begin{aligned}
4\epsilon^2 &\geq (1+\mu)\|h\|_2^2 \\
&\quad -\mu\left[\left(s^{\frac{1}{2}}+2^{\frac{1}{r}-1}s^{\frac{1}{r}-\frac{1}{2}}\right)\left(\frac{2\epsilon\sqrt{1+(s-1)\mu}}{p}+\frac{2^{\frac{1}{r}-1}\mu N^{\frac{1}{2}}\alpha^{\frac{1}{r}}s^{\frac{1}{2}}}{p}\|h\|_2\right)+2^{\frac{1}{r}-1}N^{\frac{1}{2}}\alpha^{\frac{1}{r}}\|h\|_2\right]^2 \\
&= (1+\mu)\|h\|_2^2-\frac{\mu}{p^2}\Big[4\left(1+2^{\frac{1}{r}-1}s^{\frac{1}{r}-1}\right)^2\epsilon^2 q+\left(2^{\frac{1}{r}-1}N^{\frac{1}{2}}\alpha^{\frac{1}{r}}(1+\mu)\right)^2\|h\|_2^2 \\
&\qquad +2^{\frac{1}{r}+1}N^{\frac{1}{2}}\alpha^{\frac{1}{r}}\epsilon\sqrt{q}\left(1+2^{\frac{1}{r}-1}s^{\frac{1}{r}-1}\right)(1+\mu)\|h\|_2\Big]. \qquad (5.11)
\end{aligned}
$$

By basic calculations, we can get

$$
\begin{aligned}
&(1+\mu)\left[p^2-2^{\frac{2}{r}-2}\alpha^{\frac{2}{r}}N(\mu^2+\mu)\right]\|h\|_2^2 \\
&\quad -2^{\frac{1}{r}+1}N^{\frac{1}{2}}\alpha^{\frac{1}{r}}\epsilon(1+\mu)\mu\sqrt{\hat{q}}\|h\|_2-4(p^2+\mu\hat{q})\epsilon^2\leq 0. \qquad (5.12)
\end{aligned}
$$

For the convenience of simplification, define

$$
\begin{aligned}
F(x) &= (1+\mu)\left[p^2-2^{\frac{2}{r}-2}\alpha^{\frac{2}{r}}N(\mu^2+\mu)\right]x^2 \\
&\quad -2^{\frac{1}{r}+1}N^{\frac{1}{2}}\alpha^{\frac{1}{r}}\epsilon(1+\mu)\mu\sqrt{\hat{q}}x-4(p^2+\mu\hat{q})\epsilon^2 \qquad (5.13)
\end{aligned}
$$

with $x\geq 0$. Hence, (5.12) turns into

$$
F(\|h\|_2)\leq 0. \qquad (5.14)
$$

Furthermore, it is not hard to see that

$$
1+\mu>0,\quad -2^{\frac{1}{r}+1}N^{\frac{1}{2}}\alpha^{\frac{1}{r}}\epsilon(1+\mu)\mu\sqrt{\hat{q}}<0,\quad -4(p^2+\mu\hat{q})\epsilon^2<0. \qquad (5.15)
$$

Thence, for it is useful for us to discuss $F(x)$, we consider the value of $p^2-2^{2/r-2}\alpha^{2/r}N(\mu^2+\mu)$. From the definition of p, it results in

$$
\begin{aligned}
p^2-2^{\frac{2}{r}-2}\alpha^{\frac{2}{r}}N(\mu^2+\mu) &= 1-2\left(s-1+2^{\frac{1}{r}-1}s^{\frac{1}{r}}\right)\mu \\
&\quad +\left(s-1+2^{\frac{1}{r}-1}s^{\frac{1}{r}}\right)^2\mu^2-2^{\frac{2}{r}-2}\alpha^{\frac{2}{r}}N(\mu^2+\mu) \\
&= \left[\left(s-1+2^{\frac{1}{r}-1}s^{\frac{1}{r}}\right)^2-2^{\frac{2}{r}-2}\alpha^{\frac{2}{r}}N\right]\mu^2 \\
&\quad -\left[2\left(s-1+2^{\frac{1}{r}-1}s^{\frac{1}{r}}\right)+2^{\frac{2}{r}-2}\alpha^{\frac{2}{r}}N\right]\mu+1. \qquad (5.16)
\end{aligned}
$$

We define again

$$
\begin{aligned}
G(x) &= \left[\left(s-1+2^{\frac{1}{r}-1}s^{\frac{1}{r}}\right)^2-2^{\frac{2}{r}-2}\alpha^{\frac{2}{r}}N\right]x^2 \\
&\quad -\left[2\left(s-1+2^{\frac{1}{r}-1}s^{\frac{1}{r}}\right)+2^{\frac{2}{r}-2}\alpha^{\frac{2}{r}}N\right]x+1 \qquad (5.17)
\end{aligned}
$$

with $0<x<1$. Thereupon, we get

$$
p^2-2^{\frac{2}{r}-2}\alpha^{\frac{2}{r}}N(\mu^2+\mu)=G(\mu). \qquad (5.18)
$$

Put $G(x)=0$, it leads to

$$
x=\left\{2\left[\left(s-1+2^{\frac{1}{r}-1}s^{\frac{1}{r}}\right)^2-2^{\frac{2}{r}-2}\alpha^{\frac{2}{r}}N\right]\right\}^{-1}
$$

$$
\begin{aligned}
&\times \left\{ 2\left(s-1+2^{\frac{1}{r}-1}s^{\frac{1}{r}}\right)+2^{\frac{2}{r}-2}\alpha^{\frac{2}{r}}N \right. \\
&\quad \pm \left\{ \left[2\left(s-1+2^{\frac{1}{r}-1}s^{\frac{1}{r}}\right)+2^{\frac{2}{r}-2}\alpha^{\frac{2}{r}}N\right]^2 \right. \\
&\qquad \left. \left. -4\left[\left(s-1+2^{\frac{1}{r}-1}s^{\frac{1}{r}}\right)^2-2^{\frac{2}{r}-2}\alpha^{\frac{2}{r}}N\right] \right\}^{\frac{1}{2}} \right\} \\
&= \left[\left(s-1+2^{\frac{1}{r}-1}s^{\frac{1}{r}}\right)^2-2^{\frac{2}{r}-2}\alpha^{\frac{2}{r}}N\right]^{-1} \\
&\quad \times \left\{ \left(s-1+2^{\frac{1}{r}-1}s^{\frac{1}{r}}\right)+2^{\frac{2}{r}-3}\alpha^{\frac{2}{r}}N \right. \\
&\qquad \left. \pm \left[2^{\frac{2}{r}-2}\alpha^{\frac{2}{r}}N\left(s+2^{\frac{1}{r}-1}s^{\frac{1}{r}}\right)+2^{\frac{4}{r}-6}\alpha^{\frac{4}{r}}N^2\right]^{\frac{1}{2}} \right\}. \qquad (5.19)
\end{aligned}
$$

Through the curves of the functions (2.4) and (5.19) (see Fig. 5.1, where $\alpha = 0.2$ and $N = 128$ which satisfies $\alpha^{1/r}N^{1/2} < 1$), we can obtain

$$
\begin{aligned}
&\left[\left(s-1+2^{\frac{1}{r}-1}s^{\frac{1}{r}}\right)^2-2^{\frac{2}{r}-2}\alpha^{\frac{2}{r}}N\right]^{-1} \\
&\quad \times \left\{ \left(s-1+2^{\frac{1}{r}-1}s^{\frac{1}{r}}\right)+2^{\frac{2}{r}-3}\alpha^{\frac{2}{r}}N-\left[2^{\frac{2}{r}-2}\alpha^{\frac{2}{r}}N\left(s+2^{\frac{1}{r}-1}s^{\frac{1}{r}}\right)+2^{\frac{4}{r}-6}\alpha^{\frac{4}{r}}N^2\right]^{\frac{1}{2}} \right\} \\
&=: \kappa(s;r,\alpha,N) < \frac{1}{s-1+2^{\frac{1}{r}-1}s^{\frac{1}{r}}} < \left[\left(s-1+2^{\frac{1}{r}-1}s^{\frac{1}{r}}\right)^2-2^{\frac{2}{r}-2}\alpha^{\frac{2}{r}}N\right]^{-1} \\
&\quad \times \left\{ \left(s-1+2^{\frac{1}{r}-1}s^{\frac{1}{r}}\right)+2^{\frac{2}{r}-3}\alpha^{\frac{2}{r}}N+\left[2^{\frac{2}{r}-2}\alpha^{\frac{2}{r}}N\left(s+2^{\frac{1}{r}-1}s^{\frac{1}{r}}\right)+2^{\frac{4}{r}-6}\alpha^{\frac{4}{r}}N^2\right]^{\frac{1}{2}} \right\} \\
&=: \theta(s;r,\alpha,N). \qquad (5.20)
\end{aligned}
$$

Combining with (5.18), (5.19) and the fact that

$$
\left(s-1+2^{\frac{1}{r}-1}s^{\frac{1}{r}}\right)^2-2^{\frac{2}{r}-2}\alpha^{\frac{2}{r}}N>0, \quad s>1, \quad \alpha^{\frac{1}{r}}N^{\frac{1}{2}}<1,
$$

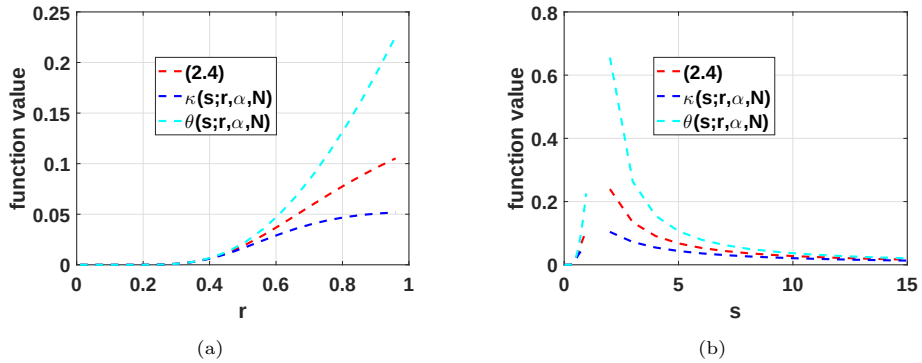

(a) (b)

Fig. 5.1. Comparison of the magnitudes of three functions $\kappa(s;r,\alpha,N)$, (2.4) and $\theta(s;r,\alpha,N)$ on s and r for given α and N for (a) $s = 5$, (b) $r = 3/4$.

under the condition $\mu < \kappa(s; r, \alpha, N)$, we get

$$p^2 - 2^{\frac{2}{r}-2}\alpha^{\frac{2}{r}}N(\mu^2+\mu) > 0. \tag{5.21}$$

Addressing the inequality (5.12) provided that (5.21) holds, we derive that

$$\begin{aligned}\|h\|_2 \le& \left\{(1+\mu)\left[p^2 - 2^{\frac{2}{r}-2}\alpha^{\frac{2}{r}}N(\mu^2+\mu)\right]\right\}^{-1}\\ &\times\left\{2^{\frac{1}{r}}N^{\frac{1}{2}}\alpha^{\frac{1}{r}}(1+\mu)\mu\sqrt{\hat{q}}\right.\\ &\left.+\left\{2^{\frac{2}{r}}N\alpha^{\frac{2}{r}}(1+\mu)^2\mu^2\hat{q} + 4(1+\mu)\left[p^2 - 2^{\frac{2}{r}-2}\alpha^{\frac{2}{r}}N(\mu^2+\mu)\right](p^2+\mu\hat{q})\right\}^{\frac{1}{2}}\right\}\epsilon\\ :=& C\epsilon.\end{aligned} \tag{5.22}$$

The proof is complete. □

Proof of Theorem 3.2. It follows from (5.10) that

$$\langle Ah, Ah\rangle \ge (1+\mu)\|h\|_2^2 - \mu\left[\left(s^{\frac{1}{2}} + 2^{\frac{1}{r}-1}s^{\frac{1}{r}-\frac{1}{2}}\right)\|h_S\|_2 + 2^{\frac{1}{r}-1}\alpha^{\frac{1}{r}}N^{\frac{1}{2}}\|h\|_2\right]^2. \tag{5.23}$$

By Lemma 2.2, (5.8) as well as the Hölder inequality, it results in

$$\begin{aligned}\langle Ah, Ah\rangle &= \langle h, A^\top Ah\rangle\\ &\le \|h\|_1\|A^\top Ah\|_\infty\\ &\le 2\epsilon\big(\|h_S\|_1 + \|h_{S^c}\|_1\big)\\ &\le 2\epsilon\left(s^{\frac{1}{2}}\|h_S\|_2 + \|h_{S^c}\|_r\right)\\ &\le 2\epsilon\left(s^{\frac{1}{2}}\|h_S\|_2 + \big(\|h_S\|_r^r + \alpha\|h\|_1^r\big)^{\frac{1}{r}}\right)\\ &\le 2\epsilon\left(s^{\frac{1}{2}}\|h_S\|_2 + 2^{\frac{1}{r}-1}\big(\|h_S\|_r + \alpha^{\frac{1}{r}}\|h\|_1\big)\right)\\ &\le 2\epsilon\left[\left(s^{\frac{1}{2}} + 2^{\frac{1}{r}-1}s^{\frac{1}{r}-\frac{1}{2}}\right)\|h_S\|_2 + 2^{\frac{1}{r}-1}\alpha^{\frac{1}{r}}N^{\frac{1}{2}}\|h\|_2\right].\end{aligned} \tag{5.24}$$

By (2.6), (5.23) and (5.24), we get

$$\begin{aligned}&2\epsilon\left[\left(s^{\frac{1}{2}} + 2^{\frac{1}{r}-1}s^{\frac{1}{r}-\frac{1}{2}}\right)\left(\frac{2\epsilon\sqrt{s}}{p} + \frac{2^{\frac{1}{r}-1}\mu N^{\frac{1}{2}}\alpha^{\frac{1}{r}}s^{\frac{1}{2}}\|h\|_2}{p}\right) + 2^{\frac{1}{r}-1}\alpha^{\frac{1}{r}}N^{\frac{1}{2}}\|h\|_2\right]\\ &\ge (1+\mu)\|h\|_2^2 - \mu\left[\left(s^{\frac{1}{2}} + 2^{\frac{1}{r}-1}s^{\frac{1}{r}-\frac{1}{2}}\right)\left(\frac{2\epsilon\sqrt{s}}{p} + \frac{2^{\frac{1}{r}-1}\mu N^{\frac{1}{2}}\alpha^{\frac{1}{r}}s^{\frac{1}{2}}\|h\|_2}{p}\right)\right.\\ &\qquad\left. + 2^{\frac{1}{r}-1}\alpha^{\frac{1}{r}}N^{\frac{1}{2}}\|h\|_2\right]^2\\ &\ge (1+\mu)\|h\|_2^2 - \frac{\mu}{p^2}\left[4\epsilon^2\left(s^{\frac{1}{2}} + 2^{\frac{1}{r}-1}s^{\frac{1}{r}-\frac{1}{2}}\right)^2 + 2^{\frac{1}{r}+1}N^{\frac{1}{2}}\alpha^{\frac{1}{r}}(1+\mu)\epsilon\|h\|_2\right.\\ &\qquad\left. + 2^{\frac{2}{r}-2}N\alpha^{\frac{2}{r}}(1+\mu)^2\|h\|_2^2\right].\end{aligned} \tag{5.25}$$

By simplifying and organizing, we get

$$\begin{aligned}&(1+\mu)\left[p^2-2^{\frac{2}{r}-2}\alpha^{\frac{2}{r}}N(\mu^2+\mu)\right]\|h\|_2^2-2^{\frac{1}{r}}N^{\frac{1}{2}}\alpha^{\frac{1}{r}}\epsilon(1+\mu)(2\mu+p)\|h\|_2\\&-4\left(s+2^{\frac{1}{r}-1}s^{\frac{1}{r}}\right)\left[\mu\left(s+2^{\frac{1}{r}-1}s^{\frac{1}{r}}\right)+1\right]\epsilon^2\leq 0.\end{aligned}\tag{5.26}$$

In addition, it is easy to see that

$$\begin{aligned}&1+\mu>0,\\&-2^{\frac{1}{r}}N^{\frac{1}{2}}\alpha^{\frac{1}{r}}\epsilon(1+\mu)(2\mu+p)<0,\\&-4\left(s+2^{\frac{1}{r}-1}s^{\frac{1}{r}}\right)\left[\mu\left(s+2^{\frac{1}{r}-1}s^{\frac{1}{r}}\right)+1\right]\epsilon^2<0.\end{aligned}\tag{5.27}$$

It is from the proof of Theorem 3.1 that when μ fulfills $\mu<\kappa(s;r,\alpha,N)$, (5.21) is satisfied. Solving the inequality (5.26) in the case of the condition $\mu<\kappa(s;r,\alpha,N)$, we gain that

$$\begin{aligned}\|h\|_2\leq&\left\{(1+\mu)\left[p^2-2^{\frac{2}{r}-2}\alpha^{\frac{2}{r}}N(\mu^2+\mu)\right]\right\}^{-1}\\&\times\left\{2^{\frac{1}{r}-1}N^{\frac{1}{2}}\alpha^{\frac{1}{r}}(1+\mu)(2\mu+p)\right.\\&\quad+\left\{2^{\frac{2}{r}-2}N\alpha^{\frac{2}{r}}(1+\mu)^2(2\mu+p)^2+4(1+\mu)\left[p^2-2^{\frac{2}{r}-2}\alpha^{\frac{2}{r}}N(\mu^2+\mu)\right]\right.\\&\qquad\left.\left.\times\left(s+2^{\frac{1}{r}-1}s^{\frac{1}{r}}\right)\left[\mu\left(s+2^{\frac{1}{r}-1}s^{\frac{1}{r}}\right)+1\right]\right\}^{\frac{1}{2}}\right\}\epsilon:=D\epsilon.\end{aligned}\tag{5.28}$$

The proof is finished. □

6. Conclusion

In this article, we prove the capability assurance of weighted $\ell_r-\ell_1$ minimization for reconstructing s-sparse vectors that are probably corrupted by disturbance. This work to a certain degree stuffs in the gap of coherence, which is one of forceful theoretical means, to compose adequate assumptions for non-convex weighted $\ell_r-\ell_1$ minimization approach to exactly/stably reconstruct s-sparse vectors. Observe that our present contribution exclusively composes of relaxed reconstruction condition and the corresponding upper bound estimation of reconstruction error. We will investigate and obtain the tighter condition even optimal ones in the future.

Acknowledgments. The authors would like to thank the referees for their valuable comments.

The work was supported in part by the National Natural Science Foundation of China (Grant Nos. 12101454, 12101512, 12071380, 62063031), by the Chongqing Normal University Foundation Project (Grant No. 23XLB013), by the Fuxi Scientific Research Innovation Team of Tianshui Normal University (Grant No. FXD2020-03), by the National Natural Science Foundation of China (Grant No. 12301594), by the China Postdoctoral Science Foundation (Grant No. 2021M692681), by the Natural Science Foundation of Chongqing, China (Grant No. cstc2021jcyj-bshX0155), by the Fundamental Research Funds for the Central Universities (Grant No. SWU120078), by the Natural Science Foundation of Gansu Province (Grant No. 21JR1RE292), by the College Teachers Innovation Foundation of Gansu Province (Grant No. 2023B-132), by the Joint Funds of the Natural Science Innovation-driven development of

Chongqing (Grant No. 2023NSCQ-LZX0218) and by the Chongqing Talent Project (Grant No. cstc2021ycjh-bgzxm0015).

References

[1] T. Cai, L. Wang, and G. Xu, Stable recovery of sparse signals and an oracle inequality, *IEEE Trans. Inf. Theory*, **56**:7 (2010), 3516–3522.

[2] Y. Cai, Weighted $l_p - l_1$ minimization methods for block sparse recovery and rank minimization, *Anal. Appl.*, **19**:2 (2021), 343–361.

[3] E.J. Candès and T. Tao, Decoding by linear programming, *IEEE Trans. Inf. Theory*, **51**:12 (2005), 4203–4215.

[4] E.J. Candès and T. Tao, The Dantzig selector: Statistical estimation when p is much larger than n, *Ann. Statist.*, **35**:6 (2007), 2313–2351.

[5] R. Chartrand, Exact reconstruction of sparse signals via nonconvex minimization, *IEEE Signal Process. Lett.*, **14**:10 (2007), 707–710.

[6] R. Chartrand and V. Staneva, Restricted isometry properties and nonconvex compressive sensing, *Inverse Problems*, **24**:3 (2008), 035020.

[7] S. Chen, D.L. Donoho, and M.A. Saunders, Atomic decomposition by basis pursuit, *SIAM Rev.*, **43**:1 (2001), 129–159.

[8] D.L. Donoho, Compressed sensing, *IEEE Trans. Inf. Theory*, **52**:4 (2006), 1289–1306.

[9] D.L. Donoho, M. Elad, and V.N. Temlyakov, Stable recovery of sparse overcomplete representations in the presence of noise, *IEEE Trans. Inf. Theory*, **52**:1 (2006), 6–18.

[10] D.L. Donoho and X. Huo, Uncertainty principles and ideal atomic decomposition, *IEEE Trans. Inf. Theory*, **47**:7 (2001), 2845–2862.

[11] H. Ge, W. Chen, and M.K. Ng, On recovery of sparse signals with prior support information via weighted ℓ_p-minimization, *IEEE Trans. Inf. Theory*, **67**:11 (2021), 7579–7595.

[12] Z. He, H. He, X. Liu, and J. Wen, An improved sufficient condition for sparse signal recovery with minimization of L1-L2, *IEEE Signal Process. Lett.*, **29** (2022), 907–911.

[13] W. Kong, J. Wang, W. Wang, and F. Zhang, Enhanced block-sparse signal recovery performance via truncated ℓ_2/ℓ_{1-2} minimization, *J. Comput. Math.*, **38**:3 (2020), 437–451.

[14] M. Lai, Y. Xu, and W. Yin, Improved iteratively reweighted least squares for unconstrained smoothed ℓ_q minimization, *SIAM J. Numer. Anal.*, **51**:2 (2013), 927–957.

[15] Y. Li and W. Chen, The high order block RIP condition for signal recovery, *J. Comput. Math.*, **37**:1 (2018), 61–75.

[16] J. Lin and S. Li, Block sparse recovery via mixed l_2/l_1 minimization, *Acta Math. Sin. Engl. Ser.*, **29**:7 (2013), 1401–1412.

[17] J. Lin and S. Li, Restricted q-isometry properties adapted to frames for nonconvex l_q-analysis, *IEEE Trans. Inf. Theory*, **62**:8 (2016), 4733–4747.

[18] J.A. Tropp, Greed is good: Algorithmic results for sparse approximation, *IEEE Trans. Inf. Theory*, **50**:10 (2004), 2231–2242.

[19] J.A. Tropp, I.S. Dhillon, R.W. Heath, and T. Strohmer, Designing structured tight frames via an alternating projection method, *IEEE Trans. Inf. Theory*, **51**:1 (2005), 188–209.

[20] W. Wang, J. Wang, Y. Wang, and Z. Zhang, A coherence theory of nonconvex block-sparse compressed sensing, *Sci. China*, **46**:3 (2016), 376–390.

[21] W. Wang, F. Zhang, Z. Wang, and J. Wang, Coherence-based robust analysis of basis pursuit de-noising and beyond, *IEEE Access*, **7** (2019,) 173216–173229.

[22] Z. Wang, A.C. Bovik, H.R. Sheikh, and E.P. Simoncelli, Image quality assessment: From error visibility to structural similarity, *IEEE Trans. Image Process.*, **13**:4 (2004), 600–612.

[23] L. Welch, Lower bounds on the maximum cross correlation of signals, *IEEE Trans. Inf. Theory*, **20**:3 (1974), 397–399.

[24] F. Wen, P. Liu, Y. Liu, R. Qiu, and W. Yu, Robust sparse recovery in impulsive noise via ℓ_p-ℓ_1 optimization, *IEEE Trans. Signal Process.*, **65**:1 (2016), 105–118.

[25] F. Wen, R. Ying, P. Liu, and R. Qiu, Robust PCA using generalized nonconvex regularization, *IEEE Trans. Circuits Syst. Video Technol.*, **30**:6 (2019), 1497–1510.

[26] J. Wen, J. Weng, C. Tong, C. Ren, and Z. Zhou, Sparse signal recovery with minimization of 1-norm minus 2-norm, *IEEE Trans. Veh. Technol.*, **68**:7 (2019), 6847–6854.

[27] Z. Xu, Deterministic sampling of sparse trigonometric polynomials, *J. Complexity*, **27**:2 (2011), 133–140.

[28] J. Zhang and S. Zhang, Recovery analysis for block $\ell_p - \ell_1$ minimization with prior support information, *Int. J. Wavelets Multiresolut. Inf. Process.*, **20**:4 (2022), 2150057.

[29] R. Zhang and S. Li, Optimal RIP bounds for sparse signals recovery via ℓ_p minimization, *Appl. Comput. Harmon. Anal.*, **47**:3 (2019), 566–584.

[30] Z. Zhou, RIP Analysis for the weighted $\ell_r - \ell_1$ minimization method, *Signal Process.*, **202** (2023), 108754.

[31] Z. Zhou and J. Yu, A new nonconvex sparse recovery method for compressive sensing, *Front. Appl. Math. Stat.*, **5** (2019), 14.